

We are IntechOpen, the world's leading publisher of Open Access books Built by scientists, for scientists

6,900

Open access books available

185,000

International authors and editors

200M

Downloads

Our authors are among the

154

Countries delivered to

TOP 1%

most cited scientists

12.2%

Contributors from top 500 universities



WEB OF SCIENCE™

Selection of our books indexed in the Book Citation Index
in Web of Science™ Core Collection (BKCI)

Interested in publishing with us?
Contact book.department@intechopen.com

Numbers displayed above are based on latest data collected.
For more information visit www.intechopen.com



Spin-Helical Dirac Fermions in 3D Topological Insulator Quantum Wires

Romain Giraud and Joseph Dufouleur

Additional information is available at the end of the chapter

<http://dx.doi.org/10.5772/intechopen.76152>

Abstract

The next generation of electronic devices based on 3D topological insulators will be developed from advanced functional nanostructures and heterostructures. Toward this goal, single-crystalline nanowires offer interesting opportunities for new developments due to the strong quantum confinement of spin-helical surface Dirac fermions and to the possibility to realize core-shell lateral nanostructures adapted to the control of the electro-chemical potential at the interface with a topological insulator. Here, we review the specific transport properties of 3D topological insulator quantum wires and the influence of disorder. Having a large energy quantization, weakly-coupled Dirac surface modes are prone to quasi-ballistic transport, with some analogies to carbon nanotubes but with spin-textured quantum states weakly coupled by non-magnetic disorder. Due to a small interaction with their environment, these surface modes are good candidates to realize novel quantum spintronic devices, spanning from ballistic spin conductors to localized spin filters. A specific topological mode also holds promises to control chiral edge states and Majorana bound states in truly 1D quantum wires, being tunable with a magnetic field or an electrical gate. Challenges toward these goals are briefly discussed, as well as the need for novel functional heterostructures.

Keywords: 3D topological insulators, nanostructures, quantum confinement, Dirac fermions, spin transport, disorder, core-shell heterostructures

1. Introduction

The topology of electronic band structures in crystals can have profound consequences at their interfaces with materials having a trivial topology, resulting in novel electronic states in reduced dimension [1, 2]. A striking example is the realization of gapless metallic states with a Dirac band

structure at the interface between two insulators, if one is a topological insulator (TI). For a 2D crystal, these are dissipationless 1D spin-helical edge states, an electronic phase known as the quantum spin Hall state [3–5]. For a 3D crystal, the metallic phase develops as 2D surface/interface states [6, 7] with a spin-helical band structure that limits their scattering by non-magnetic disorder [8]. This novel type of insulators was discovered in materials having a strong spin-orbit coupling (broken rotational symmetry) and a Hamiltonian invariant by time-reversal symmetry (TRS), belonging to the so-called \mathbb{Z}_2 topological class [7, 9]. The spin-orbit interaction can lead to a band inversion that gives rise to novel quasi-particles having a Dirac-like band structure with spin-momentum locking, at the interface with a trivial insulator (i.e., with non-inverted bands) where the energy gap must close (see **Figure 1a**). A remarkable property is that such metallic states always exist (no gap), even in the presence of perturbations, as long as the main symmetries are preserved. Thus, regardless the strength of a non-magnetic disorder, the condition for strong (Anderson) localization is never fulfilled. Still, an electronic gap (an important property for the operation of classical electronic devices) can be created, for instance by using a perturbation breaking TRS or by coupling topological states at opposite interfaces. The non-trivial nature of such gapped topological states further gives rise to novel exotic phases with a lower dimension (Majorana bound states [10] and quantum anomalous Hall state [11]) of particular interest for the quantum manipulation of coherent states weakly coupled to their environment.

The importance of topological insulators also comes from that they represent a promising alternative to conventional semi-conducting hetero-structures with, in principle, a reduced complexity on the materials' side and an increased stability of their electronic phases (over a large range of physical parameters: temperature, magnetic field, chemical potential, and disorder/inhomogeneities). The most striking example came with the discovery of the quantum spin Hall edge states in a 2D topological insulator, first evidenced with HgCdTe quantum wells [12]. This novel electronic phase shares some similarities with the magnetic-field induced integer quantum Hall state in high-mobility low-density 2D electron gases (2DEGs) of massive quasi-particles but was predicted in zero field [3, 4, 13] (no magnetic-field induced

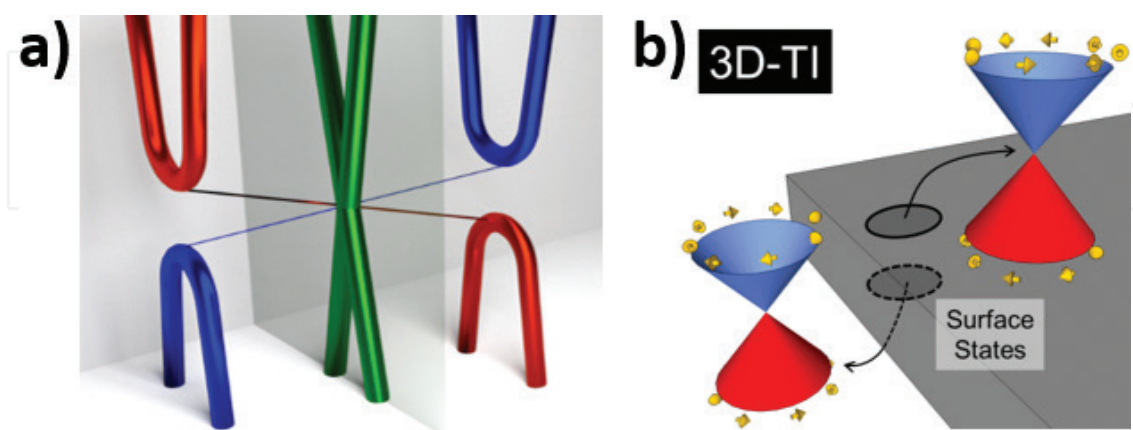


Figure 1. (a) Evolution of the band gap between a trivial insulator and a 3D topological insulator (with an inverted bulk band structure). At the interface, the gap closes and metallic states with a linear dispersion form. (b) These interface/surface states are 2D spin-helical Dirac fermions, with opposite spin helicity for opposite surfaces (the simplest case of a single Dirac cone in the center of the Brillouin zone is sketched).

orbital effect). Another important discovery was that of 3D topological insulators [14–16], which realize a 2D electron gas of massless Dirac fermions (different from those in graphene due to their helical spin texture) at the surfaces/interfaces of a *single* crystalline film (**Figure 1b**), whereas the creation of a charge-accumulation 2D gas of massive quasi-particles in conventional semiconductors often requires a more complex stacking of epitaxial layers of materials with different energy gaps and electronic-band offsets. In practice, the control of surface electronic states in a 3D topological insulator also requires that of band bending at interfaces (due to charge transfer from the environment) and a significant limitation to investigate topological surface-state transport came from that most materials are not true bulk insulators. Still, an important difference with massive quasi-particles in semiconductors, or Dirac fermions in graphene, is the reduced scattering rate by disorder due to the spin-helical texture of surface Dirac fermions [8, 17]. This favors the quasi-ballistic transport of such quasi-particles, even if they directly coexist with a large density of scattering centers, and it gives a new possibility to study such a transport regime [18] that is otherwise only accessible for massive quasi-particles in rather high-mobility AlGaAs 2DEGs (for which the 2DEG is spatially separated from Coulomb scatterers). Besides, the spin-momentum locking property of the Dirac cone favors the efficient spin-charge conversion in spintronic devices [19–25], still with some potential for improvement due to the enhanced transport length [17], if interface scattering could be further reduced.

Contrary to the case of 2D TIs, with only rare examples found to date, a number of 3D TI materials were discovered, both by theory and experiments, often using *ab initio* calculations or electron spectroscopy techniques to directly unveil the Dirac band structure of topological surface states (TSS). This offered an important playground to investigate [26, 27], but it is also a source of confusion due to the diversity of these materials and the complexity of some of them. In particular, their study by charge transport measurements proved to be difficult because many materials identified as topological insulators are also semiconductors with a rather small gap, often with a large finite bulk conductivity due to disorder (electrical doping) and a strong electronic polarizability [28]. The search for large-gap 3D topological insulators remains challenging. Indeed, beyond the need for specific symmetries of the crystal structure, it is fundamental to search for materials with a band inversion. With conventional semiconductors, this inversion is usually induced by a strong intrinsic spin-orbit coupling. This is typical for materials with large-Z elements, which also have a rather small bulk energy gap induced by Coulomb interactions. This combination is therefore favorable to realize a band inversion, and since it results from opposite contributions, most Z2 topological insulators tend to have a rather small gap that barely exceeds 300 meV in most cases. Natural point defects, such as vacancies (which are thermodynamically stable and therefore always exist in crystals), can be massively present (small activation energy) and they often act as donors or acceptors, thus easily leading to metallic-like bulk properties typical of degenerate semiconductors (sometimes approaching the dirty-metal limit). Among these semiconductors, Bi-based chalcogenides play an important role for that the continuous tuning of their chemical composition, between different stoichiometric compounds, can change a trivial insulator (no band inversion) into a topological insulator (band inversion), with a varying bulk gap and a relative change of the topological Dirac degeneracy point with respect to the bulk band structure [29]. Binary 3D topological insulators, such as Bi_2Se_3 and Bi_2Te_3 , usually have a large residual

bulk conductivity (despite a very small bulk-carrier mobility), so that the total conductance of wide and/or thick nanostructures is dominated by bulk transport. This contribution is slightly reduced in Bi_2Te_3 , but only high-energy surface quasi-particles can be studied because the Dirac point lies deep into the valence band, whereas the Fermi level is pinned near or above the top of the valence band. In Bi_2Se_3 , the Dirac point lies within the bulk band gap, but the Fermi level is high above the bottom of the conduction band (due to too many Se vacancies), so that it can only be modified over a small energy range by an electrical gate (efficient electrostatic screening), unless the nanostructure is ultra thin. Ternary compounds gave the most advanced results to optimize the surface-to-bulk ratio to the conductance and this approach was successfully used to investigate surface-state transport in the quantum Hall regime at low magnetic fields (close to the Dirac point) [30]. It remains, however, difficult to prepare nanostructures (thin films, nanoribbons, and nanowires) of ternary or even quaternary materials with optimized compositions [31]. Novel heterostructures, such as core-shell nanowires, could thus be important to develop functional devices based on 3D topological insulators, not only to achieve dominant surface transport and use the spin-momentum locking property of 2D topological surface states, but also to realize novel low-dimensional quantum devices at the sub-micron scale despite disorder, due to anisotropic scattering, which are different from “conventional” mesoscopic conductors with either massive quasi-particles in semiconductors or Dirac fermions in graphene (both with quantum transport properties controlled by large-angle scattering).

Unique properties of spin-helical Dirac fermions in disordered 3D topological insulators also arise from their strong quantum confinement in narrow nanowires (quantum wires). The Dirac nature results in a large energy quantization, as compared to the confinement energy of massive quasi-particles, which further reduces their scattering by disorder and favors the quasi-ballistic transport of quasi-1D surface modes [18]. Thus, their quantized band structure gives some specific signatures of topological surface-state transport, unveiled by quantum corrections to the conductance [18, 32, 33], which can be easily distinguished from bulk transport (even for highly-degenerate semiconductors, such as Bi_2Se_3 and Bi_2Te_3). Their spin texture also contribute to reduce their coupling to the environment, so that decoherence due to electronic interactions is also further reduced. All in all, 3D topological insulator quantum wires offer new possibilities to investigate mesoscopic transport in the quasi-ballistic regime over a large range of parameters (dimensionality, aspect ratio, and disorder strength), whereas it can hardly be investigated otherwise. Rare studies based on high-mobility AlGaAs 2DEGs were limited to the near-clean limit [34, 35], with little possibilities to modify some important physical parameters, such as disorder or the kinetic energy, over a broad range. Disordered semiconducting or metallic nanowires are always diffusive conductors. Disordered semiconducting or metallic nanowires are always diffusive conductors. Most similar systems are actually carbon nanotubes, which are clean systems with ballistic-transport properties and very large confinement energies. Disordered 3D TI quantum wires represent an intermediate situation that corresponds to quasi-ballistic transport (due to anisotropic scattering rather than to a weak disorder) and their quantized surface states can be manipulated with rather small magnetic fields, due to larger diameters than for carbon nanotubes. As a consequence, the specific properties of quantized surface Dirac modes can be revealed by the study of different quantum corrections to the conductance (Aharonov-Bohm oscillations and non-universal conductance fluctuations), with good statistical information obtained from magneto-transport measurements below 15 T [18].

2. Transport properties of 2D topological surface states

To understand the physics of 3DTI quantum wires, it is first necessary to take a closer look at the scattering of 2D spin-helical Dirac fermions by a non-magnetic disorder. In this case, backscattering is not suppressed since it remains possible by successive small-angle scattering events, over a scale given by the transport length, l_{tr} . However, the spin texture favors forward scattering, so that the transport length of topological surface state is largely enhanced with respect to the disorder correlation length. As a consequence, the condition for ballistic transport can already be realized in nanostructures with dimensions smaller than a micron, and quantum devices with a simple geometry can be built from individual nanowires.

2.1. Nanostructures of 3D topological insulators for surface-transport studies

Due to their residual bulk doping, the study of surface-state transport in disordered 3D topological insulators is not straightforward. Considering the case of a highly-degenerate semiconductor, such as Bi_2Se_3 , with a bulk carrier density as high as $5 \cdot 10^{19} \text{ cm}^{-3}$ (which roughly corresponds to about 1% of Se vacancies, acting as double donors), the cross over thickness t_c for which the surface conductance becomes comparable to the bulk conductance is roughly given by $t_c = 2(n_s \mu_s)/(n_b \mu_b)$. For a strong disorder typical for Bi_2Se_3 , common to both surface and bulk states, the mobility of topological surface states is about one order of magnitude larger than that of bulk states (enhancement due to the anisotropic scattering of spin-helical Dirac fermions) [17]. Taking band bending into account [36], typical values for the surface and bulk carrier densities are $n_s = 5 \cdot 10^{12} \text{ cm}^{-2}$ and $n_b = 5 \cdot 10^{19} \text{ cm}^{-3}$. This gives a value $t_c = 20 \text{ nm}$. Based on a realistic approximation (ignoring details of band bending due to a very short Thomas-Fermi screening length $\lambda_{TF} \lesssim 3 \text{ nm}$), this lower bound for t_c (which is likely be larger for smaller bulk carrier densities) clearly shows that the control of topological surface-state transport in disordered 3D TIs requires the use of thin nanostructures. These were successfully grown by different bottom-up methods, each technique having both advantages and disadvantages. Ultra-thin layers of high quality can be prepared by molecular beam epitaxy and are well adapted to tune the interface band structure by electrical fields, but films thicker than 20 nm tend to grow 3D and have more defects. High-quality single-crystalline nanostructures with large aspect ratios can be grown by catalyst-assisted molecular-beam epitaxy or chemical vapor deposition, as well as by catalyst-free vapor transport, but ultra-thin structures are seldom. Very narrow quantum wires can also be prepared by electrodeposition in nanomembranes, presently with some intrinsic limitations related to small diameter fluctuations in ultimate nanomembranes that give quantum confinement inhomogeneities. In all cases, individual nanostructures stable in air can be randomly grown on or transferred onto SiO_2/Si substrates, appropriate to create an electric field at the interface by applying a backgate voltage.

In our work, we mostly investigated the charge transport properties of *single-crystalline atomic-flat Bi_2Se_3 and Bi_2Te_3 nanostructures* grown by catalyst-free vapor transport (**Figure 2a**), with *faceted* shapes of different aspect ratios (nanoplatelets, nanoribbons, nanowires; **Figure 2b**) [37]. As explained below, this allowed us to study the physics of spin-helical Dirac fermions in 2D or in 1D, that is, without or with quantum confinement, respectively. Despite strong disorder, it was shown that momentum scattering is reduced in all cases, due to the spin texture (2D surface states) and quantum confinement (1D surface modes). This has important consequences for both spin transport and quantum coherent transport, as discussed in detail below.

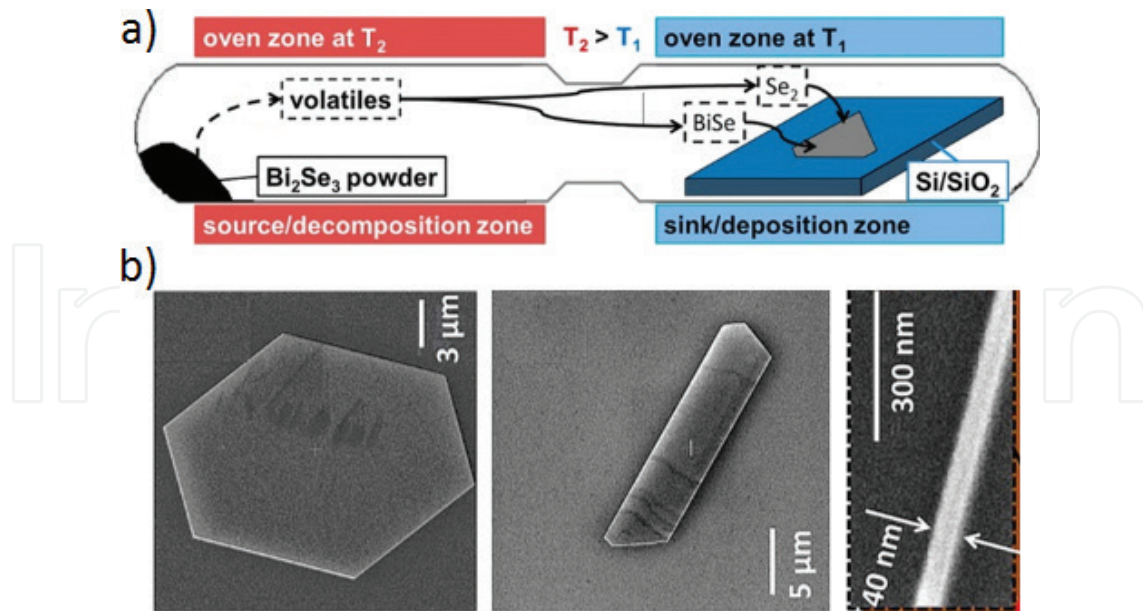


Figure 2. (a) Growth of Bi_2Se_3 nanostructures on $p^+-\text{Si}/\text{SiO}_2$ substrates by vapor transport in a closed quartz ampoule. The sublimation of Bi_2Se_3 crystals generates a flow of molecular species (BiSe and Se_2) toward the lower temperature area, where they recombine to form single crystalline nanostructures *in the plane* of the substrate. (b) Nanostructures with different aspect ratios (thin platelets, wide nanoribbons, and narrow nanowires) are distributed randomly onto amorphous SiO_2 . After [37].

2.2. Band bending and interface charge transfers

The electrical properties of 2D topological surface states can be investigated by quantum magnetotransport $G(B)$ studies and transconductance $G(V_g)$ measurements at low temperatures, which give access to all microscopic parameters (carrier density, mobility, and effective mass) for all carriers (topological interface states, topological surface states, and bulk states). A careful analysis of Shubnikov-de Haas oscillations due to the energy quantization of Landau levels in high magnetic fields gave detailed insights into the electronic band profiles in the thickness of wide Bi_2Se_3 nanostructures (nanoplatelets and nanoribbons) [36]. Important results are summarized as follows:

1. Due to the large residual bulk density and the pinning of the Fermi energy in the conduction or valence band of materials with a large dielectric constant, the bulk contribution to the conductance is never negligible.
2. Besides, it usually controls the upward band bending at interfaces of the topological insulator (charge transfer of bulk carriers to empty gapless topological surface states).
3. Downward band bending can, however, exist if a massive charge transfer from another origin is also present (surface/interface disorder, surface adsorbents, and electrostatic gate). Such a situation is more likely to happen for materials with a small bulk carrier density.
4. If the surface/interface density is very large (typically for $n_s > 10^{13} \text{ cm}^{-2}$), a Rashba charge-accumulation 2DEG of massive quasi-particles coexist with Dirac topological states.

For usual as-grown Bi_2Se_3 nanostructures exposed to air, a typical band profile is defined from the contribution of three electronic populations (bulk carriers and two topological states with

different Fermi energies), and the bulk carrier density is large enough to control charge transfer at interfaces and to induce upward band bending. Due to efficient Coulomb screening, an electrostatic gate is solely influencing the population of a single topological interface nearby, so that an independent tuning of both topological states is only achieved in dual-gate devices [38]. In a backgate geometry, the applied voltage is modifying the band bending at the bottom interface only, which results in the tuning of the electro-chemical potential of the interface topological states but not of the surface topological states since, in most cases, the electrical field is totally screened by bulk carriers nearby the bottom interface [17]. In all cases, the backgate-voltage dependence of the conductance nevertheless remains an efficient way to probe the interface topological states and study their properties by transport measurements. A striking example is shown in **Figure 3**, for a rather thick Bi_2Se_3 nanoribbon patterned in a Hall-bar geometry, with a low-enough bulk-carrier density to favor downward band bending at interfaces [36]. For a large interface carrier density, massless Dirac fermions coexist with a Rashba-type massive 2D electron gas. In this case, the back-gate voltage is changing the carrier concentration of different electronic states located at the bottom interface (shift of some peaks in the Fourier transform of Shubnikov de Haas oscillations, **Figure 3b**). The related band profile shown in **Figure 3c** is in very good quantitative agreement with a triangular potential at this interface.

2.3. Anisotropic scattering and charge transport length (=spin diffusion length)

Further important information on the scattering of spin-helical Dirac fermions by a non-magnetic disorder can be obtained from transconductance $G_{(V,G)}$ measurements [17]. It is indeed important to distinguish between two different scattering times and, accordingly, between two different length scales (**Figure 4a**):

1. The quantum lifetime of quasi-particles can be inferred from Shubnikov-de Haas measurements. It is associated with the mean-free path l_e between two successive scattering centers (thus to the microscopic disorder correlation length) and this momentum scattering time relates to the quantum mobility.
2. The transport time of carriers corresponds to the timescale for momentum backscattering, over a length called the transport length L_{tr} , related to the transport mobility, which determines the classical conductance. Whereas direct backscattering is forbidden by spin-momentum locking (giving dissipationless states in a 2D TI), it is allowed by multiple scattering processes in a disordered 3D TI, resulting in a finite transport length.

Using a thin Bi_2Se_3 nanoribbon (**Figure 4b**), the backgate voltage allowed us to modify the upward band bending, induced by a rather large bulk carrier density, at the bottom interface ("lower surface state", LSS). All microscopic transport parameters could be inferred from quantum magnetotransport (**Figure 4c**) and trans-conductance (**Figure 4d**) measurements [17]. Contrary to bulk carriers, for which $l_e \sim L_{tr}$ is given by the disorder correlation length ξ (isotropic scattering due to a short-range disorder potential), the transport length of both upper and lower topological surface states was found to be much larger than the mean-free path, despite a limitation at about 200 nm probably due to the finite coupling with bulk carriers [larger values are expected for decoupled topological states and/or in materials with a larger disorder correlation length, such as Bi_2Te_3].

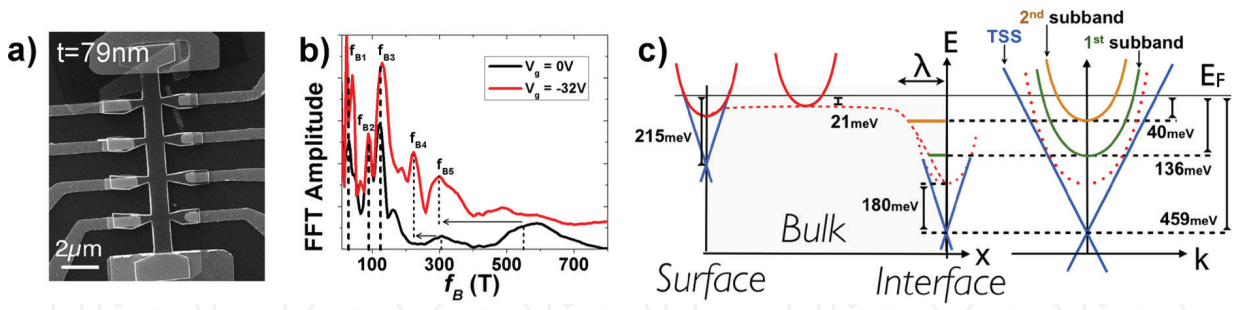


Figure 3. (a) Scanning-electron microscope image of a Hall-bar patterned Bi_2Se_3 thick nanoribbons, (b) fast-Fourier transform of the longitudinal magneto-resistance for two different back-gate voltages, and (c) evolution of the electronic band profile from the top surface to the bottom interface, typical for a low bulk-carrier density (downward band bending) and a large interface carrier density (coexistence of topological states with a Rashba 2DEG). After [36].

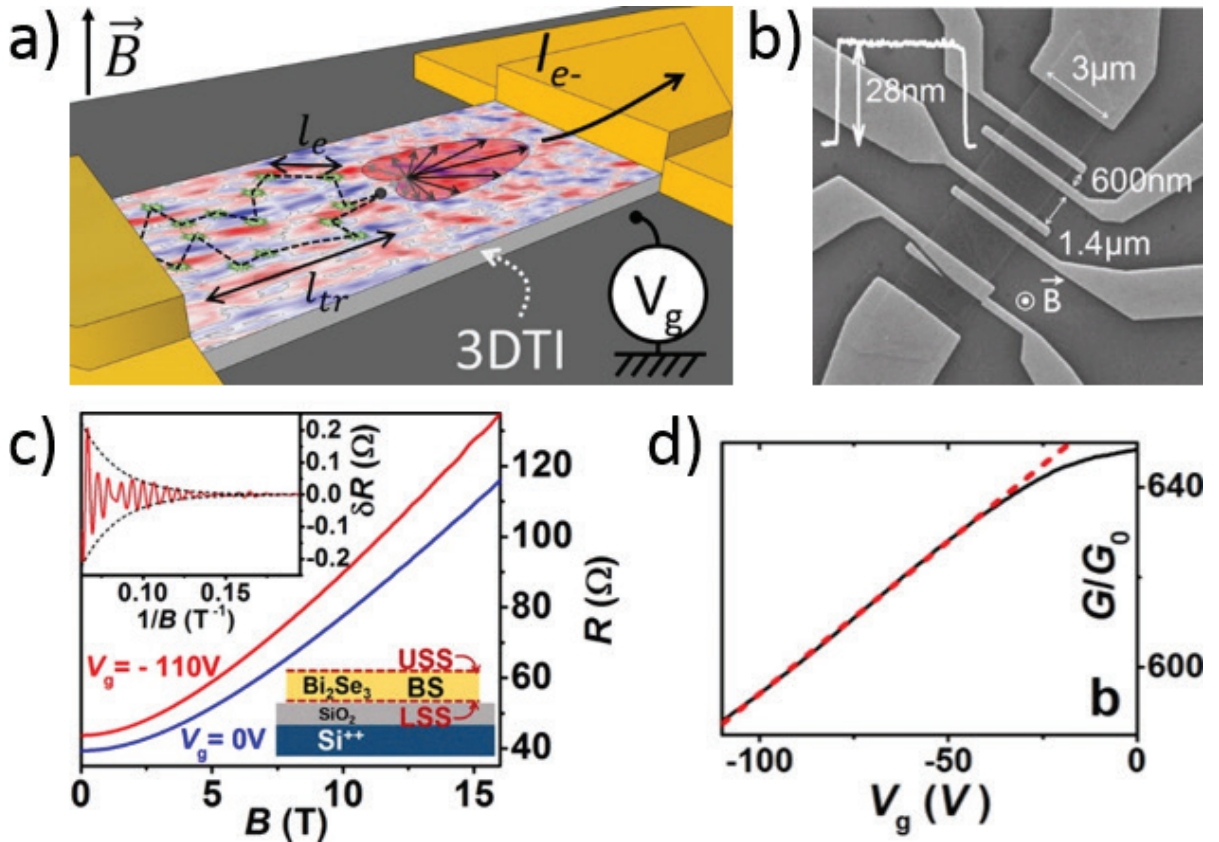


Figure 4. (a) Anisotropic scattering by disorder. The backscattering transport length L_{tr} can be much longer than the mean-free path l_e ; (b) scanning electron microscope image of a thin Bi_2Se_3 nanoribbon with traversing ohmic contacts; (c) longitudinal magneto-conductance for two different backgate voltages. Inset: Shubnikov-de Haas quantum oscillations; (d) backgate voltage dependence of the conductance and linear fit from which the transport length of the lower surface states (bottom interface) is inferred. After [17].

The average number of scattering centers involved in a backscattering process is directly related to the ratio L_{tr}/l_e and it can give some important information on the nature of both the scattering potential and the quasi-particles. Importantly, we revealed the long-range nature of disorder for spin-helical surface Dirac fermions, due to efficient electrostatic screening and

spin-momentum locking, which results in strongly anisotropic scattering, as observed by local probe microscopy. This means that forward scattering is favored for such quasi-particles and that the transport length is strongly enhanced ($L_{tr} \gg l_e$), as predicted by theory [8] and confirmed by trans-conductance measurements [17]. Such a situation never happens in other materials within which charge carriers directly coexist with disorder (including Dirac fermions in graphene), where the scattering of quasi-particles by any kind of disorder is isotropic (that is, $L_{tr} \sim l_e$). Only high-mobility AlGaAs 2DEGs can realize such a situation of anisotropic scattering. In this case, however, this is due to the spatial separation of free carriers and localized ionized donors, and it is not possible to vary the degree of disorder over a wide range, so that there is little room to investigate quasi-ballistic transport (in other words, the transition from ballistic to diffusive transport is rather abrupt and happens already when a small amount of impurities are introduced in the system). This is not the case for spin-helical Dirac fermions, and this property is at the origin of their unique transport properties, particularly in nanostructures, with an extended range of parameters to study quasi-ballistic transport, and therefore the ballistic-to-diffusive crossover in mesoscopic conductors.

This enhanced transport length for topological surface states is also important for spin transport studies, as it gives a lower limit for the size of functional spintronic devices making use of the spin-momentum locking property. Indeed, due to the strong spin-orbit coupling, there is a direct correspondence between the momentum-backscattering transport length and the spin relaxation length. With wide Bi_2Se_3 nanostructures, this scale is rather short (~ 200 nm), [17] so that, for instance, lateral spin valves could only be realized in the short-junction limit. This also shows that the true potential for the spin-to-charge conversion in highly-disordered Bi_2Se_3 could still give an improvement in the conversion efficiency by two orders of magnitude with respect to state-of-the-art records, with an inverse Edelstein length l_{IEE} determined by the intrinsic transport length of the 3D topological insulator, whereas it presently remains limited by the spin/momentum relaxation below metallic ohmic contacts (with $l_{IEE} \sim 2$ nm).

2.4. Dimensionalities of transport

The enhancement of the transport length for topological surface states also has two fundamental consequences for the quantum transport properties of 3D TI nanostructures and the dimensionality of surface charge transport:

1. The phase coherence length of TSS is also enhanced in the same ratio for diffusive 2D surface states in nanoplatelets or wide nanoribbons, so that mesoscopic transport can be studied in rather wide and long conductors (well beyond the micron size), despite relatively strong disorder. Since $L_\phi \gg L_{tr}$ (L_ϕ being determined by inelastic scattering), quantum corrections to the conductance due to diffusive phase-coherent transport can thus be revealed by magneto-transport measurements with magnetic fields as small as 100 mT.
2. The condition for ballistic transport in the transverse motion of surface carriers along the perimeter is more restrictive ($L_p < 2 L_{tr}$), but it can be fulfilled for rather long ($L_p \sim 500$ nm), and therefore with nanostructures having a large cross section ($S \sim 0.2 \mu\text{m}^2$). Contrary to the case of carbon nanotubes, magnetic flux-dependent periodic phenomena in these *quantum wires* (such as the Aharonov-Bohm interference) can therefore be studied in rather small fields, below 1 T.

In the case of highly-disordered Bi_2Se_3 nanostructures ($l_c \sim 30$ nm), large values of L_{tr} (>200 nm) [17] and of L_ϕ (>2 μm) [39] were found. This implies that the dimensionality of surface-state transport is reduced in narrow nanostructures (mostly nanowires) and that their band structure is modified due to quantum confinement (which even further reduces the scattering by disorder). It thus becomes important to distinguish between three different situations for the dimensionality of charge transport:

1. No quantum confinement [L_{tr} is shorter than every dimensions]. Surface-state transport is diffusive and quasi-particles are 2D spin-helical Dirac fermions with a continuous spin-helical Dirac-cone band structure.
2. Transverse quantum confinement [the perimeter L_p becomes shorter than $2 L_{tr}$]. Surface-transport is quasi-ballistic if the distance between contacts is longer than L_{tr} and ballistic otherwise. The length L remains much larger than L_{tr} so that surface modes are quasi-1D channels in such *long* nanowires (becoming truly 1D only when they close).
3. Full quantum confinement [all dimensions are shorter than L_{tr}]. Spin-helical Dirac fermions are then fully localized in a *short* nanowire, which becomes a 0D quantum dot.

We remark that the dimensionality of quantum coherent transport is another quantity determined by comparing the dimensions of a mesoscopic conductor to the phase coherent length L_ϕ . Since L_ϕ is longer than L_{tr} , nanoribbons with a width W , such as $L_{tr} < W < L_\phi$, have 2D spin-helical surface Dirac fermions but quantum coherent transport is 1D (which modifies the self-averaging of quantum interference in long conductors, for which the length L is longer than L_ϕ).

3. Transport properties of quasi-1D topological surface states

Signatures of the quasi-ballistic transport of topological surface states in 3D TI quantum wires can be revealed by the study of quantum corrections to the conductance. In a bulky nanostructure, spin-helical Dirac fermions propagate on the surface in a hollow-type electrical geometry, in analogy to carbon nanotubes (ballistic transport) or to the Sharvin-Sharvin metallic tubes (diffusive transport). Phase-coherent transport in the transverse direction (along the perimeter of the nanowire) thus gives rise to periodic Aharonov-Bohm oscillations in the longitudinal magnetoconductance, determined by a well-defined cross section $S = L_p^2/(4\lambda\phi)$, and their observation in wide Bi_2Te_3 nanoribbons gave the first robust evidence of surface states by transport measurements [40]. Their topological nature was then confirmed by a study of decoherence at very low temperatures in narrow (quantum) nanowires [39], which revealed the unusual weak coupling to the environment and the ballistic motion in the transverse direction. Later, phase-coherent transport in the longitudinal direction was investigated in a study of conductance fluctuations [18], which revealed the subtle influence of disorder in the quasi-ballistic regime, leading to a non-universal behavior of quantum interference. A detailed understanding of the propagation of spin-helical 1D surface modes showed that both the spin texture of Dirac fermions and their quantum confinement are responsible for the weak scattering by disorder [41], thus leading to

the weak coupling between quantum states, a necessary condition for their manipulation by radio-frequency fields, as well as for the study of specific properties related to a single topologically-protected low-energy mode, such as 1D chiral edge states or Majorana bound states [42].

3.1. Quantum confinement: 1D Dirac spectrum

In quantum wires ($L_p < 2 L_{tr}$), the surface-state band structure is modified by periodic boundary conditions imposed in the transverse direction of the nanostructure, leading to the quantization of the transverse momentum k_{\perp} (Figure 5b). This situation is equivalent to the energy quantization of quasi-particles confined into a quantum well with infinitely-high potential barriers, and for Dirac fermions, the transverse energy becomes quantized with a constant energy-level spacing $\Delta = \hbar v_F 1/L_p$ between successive transverse modes. Due to the winding of the wave function along the perimeter (curvature) and to the spin-momentum locking of helical Dirac fermions, an additional Π Berry phase suppresses the topological protection of all energy modes in zero magnetic field (pairs of gapped states). However, if a magnetic field is applied along the nanowire axis, the Aharonov-Bohm flux modifies the periodic boundary condition (which gives an overall shift of transverse quantization planes, thus tuning the energy spectrum). Importantly, this flux dependence can restore the topological protection periodically when the Aharonov-

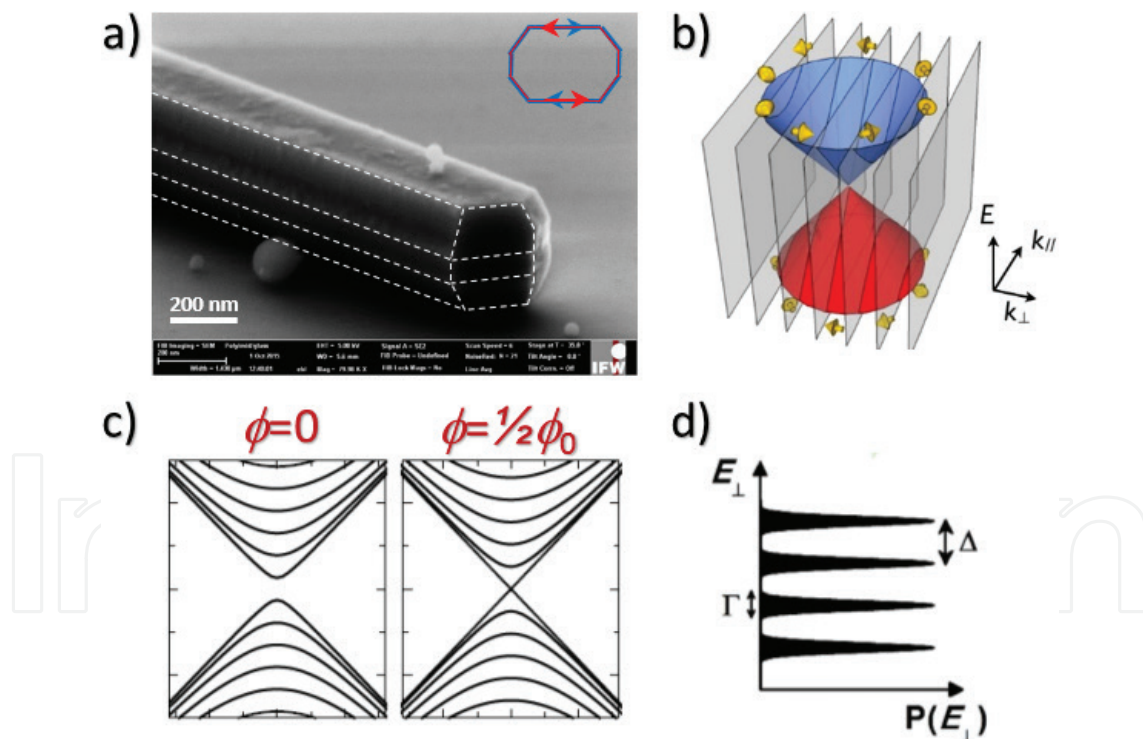


Figure 5. (a) Scanning electron microscope image of a narrow Bi₂Se₃ nanowire, with a perimeter $L_p = 300$ nm. Dashed lines separate different facets. Inset: schematics of the cross section and coherent winding of topological surface states; (b) transverse-impulse quantization planes intersecting the spin-helical Dirac cone. By applying a magnetic flux, all planes are continuously shifted in the k_{\perp} direction; (c) resulting band structures for two different values of the magnetic flux ϕ . For $\phi = 0$, quantum confinement gives pairs of modes with a finite energy gap Δ . For $\phi = 1/2\phi_0$, a single topological mode with linear dispersion appears (quantization plane intersecting the Dirac point); (d) energy broadening Γ of the quantized transverse energy due to disorder [for 3DTI quantum wires, Γ is smaller than Δ , even for relatively strong disorder].

Bohm phase compensates the curvature-induced Berry phase, giving rise to a single gapless and linear mode with perfect transmission (**Figure 5c**), independent of disorder [43].

In recent years, a couple of interesting studies suggested the influence of such a topological mode on quantum transport properties, particularly the Aharonov-Bohm (AB) oscillations [32, 33, 44]. These results raised some important questions since it was not possible to give a quantitative interpretation of the physical phenomena observed (Aharonov-Bohm oscillations and non-universal conductance fluctuations) solely based on the contribution of this perfectly transmitted mode to the conductance. In particular, the amplitude of these quantum corrections to the conductance was always found much smaller than the conductance quantum G_0 . It thus remained unclear whether these properties were a signature of a topological transition or were rather induced by all spin-textured modes, including dominant contributions from high-energy quasi-1D modes. Actually, the quantum magneto-conductance is mostly due to a limited number of modes, those partially-opened modes with a quantized transverse energy close to the Fermi energy. Since most studies were conducted in the large-N limit ($E_F \gg \Delta$), the relative contribution of the topological surface mode is therefore rather small. A full quantitative understanding required to describe the energy dependence of the transmissions for all surface modes, considering both disorder and interfaces with metallic contacts (see Section 3.4 for details). In particular, the scattering of surface modes by disorder results in the energy broadening Γ of quantized modes (**Figure 5d**). We evidenced that the quasi-ballistic regime is closely related to the condition $\Gamma \ll \Delta$, which is satisfied over an unusual broad parameters range (disorder strength, energy) in 3D topological insulator nanostructures [41].

3.2. Quantum coherence I: Aharonov-Bohm oscillations

The quantum coherent transport of topological surface states in the transverse direction of a 3D TI nanostructure results in conductance oscillations when a *longitudinal magnetic induction* B_{\parallel} is applied (hence a magnetic flux $\phi = B_{\parallel} * S_{el}$, where S_{el} is the effective electrical cross section of metallic surface states). This is due to the flux-periodic evolution of the Aharonov-Bohm quantum interference giving successive conductance maxima (constructive interference) and minima (destructive interference). Because the phase coherence length can be as large as a couple of micrometers (at very low temperatures), two different situations must be considered for coherent transport in the *transverse motion* of surface states:

1. When $L\phi \sim L_p/2$, clear periodic oscillations of the conductance are directly visible in the longitudinal magneto-conductance $G(B_{\parallel})$. In this case (wide nanoribbons), only the fundamental-harmonic Aharonov-Bohm interference modifies the conductance, a behavior which already reveals that the phase averaging due to disorder is not efficient, despite a high point-defect density in most 3DTI materials.
2. When $L\phi \gg L_p$, that is, either at very low temperatures or for short-perimeter nanowires (quantum wires), the periodic AB behavior is usually hidden in complex $G(B_{\parallel})$ traces. This is due to the multiple-harmonic contributions to the transverse quantum interference (related to the multiple winding of coherent trajectories along the perimeter), and to the influence of disorder (phase shifts). The periodic behavior can, however, be revealed by a Fourier transform analysis.

3.2.1. Case of wide nanoribbons (long-perimeter limit, with $L_\phi \sim L_p/2$)

For wide nanoribbons, periodic Aharonov-Bohm oscillations are directly visible in $G(B_{||})$ traces, with a rather small amplitude typical for the large-N limit in a mesoscopic conductor, where N is the number of populated transverse modes, with $N = E_F/2\Delta$, since $\Delta = \hbar v_F/L_p$ is smaller than E_F . As seen in **Figure 6** for a wide Bi_2Te_3 nanoribbon ($E_F \sim 120$ meV; $L_p = 940$ nm; $\Delta = 2$ meV), the Aharonov-Bohm period, $\delta B_{AB} = 150$ mT, directly relates to the electrical cross section of the nanostructure, with a value being slightly smaller than that given by its physical dimensions (the topological surface states being “buried” below a thin native oxide layer, typically 5 nm thick). The fast-Fourier transform of the $G(B_{||})$ trace thus gives a single peak at the AB frequency.

According to theory, the overall phase shift of this sine evolution due to the AB quantum interference depends on both the degree of disorder and the energy of Dirac quasi-particles [43]. In most cases, the Fermi energy is very large and AB oscillations are phase locked with a conductance maximum in zero magnetic field, as found in many experiments and confirmed by theory. Yet, theory predicts the opposite situation (conductance minimum for a zero magnetic flux) when the chemical potential is near the Dirac point. The overall energy dependence of this phase shift can be quantitatively obtained from models taking explicitly disorder into account, and it allowed us to reveal an oscillatory behavior that is directly related to quantum confinement (see Section 3.4).

For lower temperatures (longer L_ϕ) or for narrower nanoribbons, roughly when $L_\phi \sim L_p$, additional Altshuler-Aronov-Spivak (AAS) oscillations develop in addition. These correspond to quantum interference related to the complete winding of coherent paths along the perimeter, with time-reversed coherent loops so that this contribution is never damped by disorder, which is the usual situation found in (diffusive) mesoscopic conductors.

3.2.2. Case of narrow (quantum) nanowires (short-perimeter limit, $L_p < 2 L_{tr} \ll L_\phi$)

For narrow nanostructures, the conductance modulation due to both AB and AAS interferences results from a complex mixing of high-order harmonics (multiple windings of coherent loops),

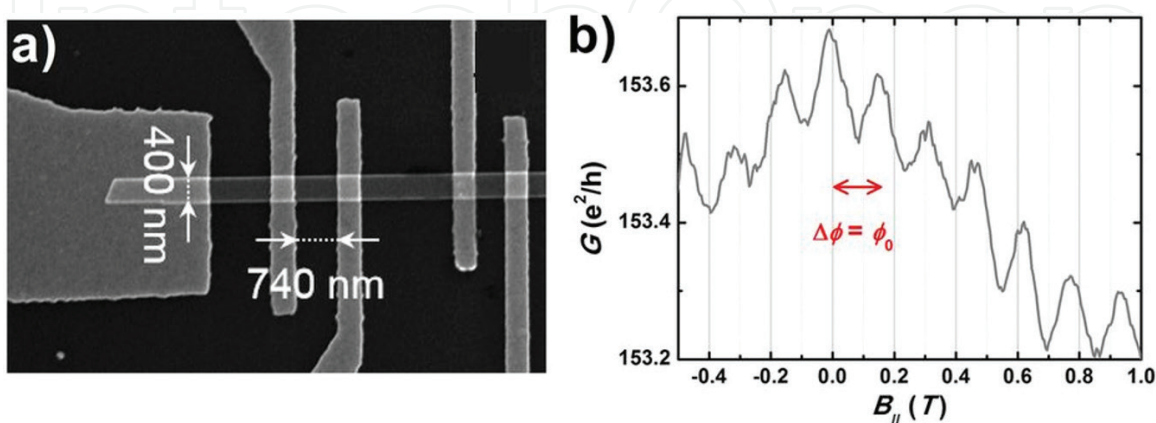


Figure 6. (a) Scanning electron microscope image of a Bi_2Te_3 nanowire with a rather large perimeter $L_p = 940$ nm (width $w = 400$ nm, height $h = 70$ nm) and ohmic CrAu contacts; (b) Aharonov-Bohm periodic oscillations (fundamental harmonics), with a period δB_{AB} that directly relates to the nanowire’s cross section. After [18].

with harmonic-dependent phase shifts induced by disorder and varying relative amplitudes due to quasi-ballistic transport. The periodic-flux dependence of the longitudinal magneto-conductance is therefore hardly visible in most $G(B_{\parallel})$ traces, though it can still be when low-order harmonics remain dominant (as shown in **Figure 7b**). Since this periodic behavior is specific to topological surface states (with a flux-periodic energy spectrum), it can always be unveiled by a careful fast-Fourier transform analysis, provided that enough oscillations are measured (that is, when the field range largely exceeds the fundamental AB period). For a micron-long Bi_2Se_3 quantum wire with perimeter $L_p = 280$ nm, up to six harmonics were clearly resolved at very low temperature, as seen in **Figure 7c**) [39].

For short wires ($L \sim L_{\phi}^{\text{BS}}$), we also remark that a complication comes further from that aperiodic conductance fluctuations due to bulk carriers coexist with surface periodic AB oscillations [although $L_{\phi}^{\text{BS}} < L_{\phi}^{\text{SS}}$, the self-averaging of coherent bulk transport is reduced at very low temperatures due to their charge transport dimensionality $d = 3$ and to longer L_{ϕ}^{BS} values]. Besides, because $G(B_{\parallel})$ curves are measured over a finite field range, the FFT of bulk aperiodic conductance fluctuations often results in a non-monotonous background, possibly giving “peaks” but with no relation to a periodic behavior, contrary to that of $G(B_{\parallel})$ changes due to the AB interference.

The ballistic nature of the transverse motion in such quantum wires results in an unusual temperature dependence of the phase coherence length L_{ϕ}^{SS} , with a $1/T$ behavior observed for all harmonics. This is the signature of both ballistic transport ($L_{\phi} = v_F \tau_{\phi}$) and a decoherence time $\tau_{\phi} \sim 1/T$ limited by a weak coupling to fluctuations of the environment [39]. All other scenarios based on decoherence limited by either the Nyquist noise or the thermal noise give a very different power-law dependence.

An extra signature of the quasi-ballistic regime is also found when considering the relative amplitude of AB harmonics. Contrary to the case of a diffusive mesoscopic conductors, their amplitudes are not increasingly small for higher orders n and they cannot be described by an exponential damping behavior related to the ratio $L_{\phi}/L_{n'}$, where $L_n = n \cdot L_p$ [39]. This is due to disorder and to both geometric and contact effects, which all influence details of the quantum interference for different quantum coherent paths, in the quasi-ballistic regime [41]. In general, it thus remains difficult to investigate details of the AB oscillations in this regime, due to the complex mixing of all harmonics in the presence of disorder, which varies for different configurations of the microscopic disorder (as obtained by thermal cycling at room temperature of a given mesoscopic conductor).

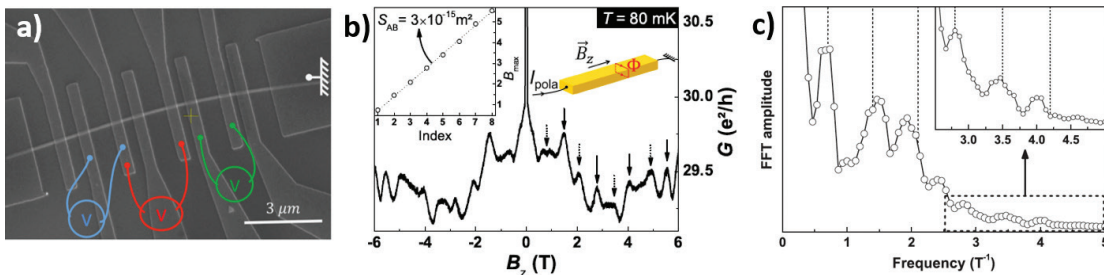


Figure 7. (a) Scanning electron microscope image of a narrow Bi_2Se_3 nanowire with a rather short perimeter $L_p = 280$ nm and ohmic Al contacts; (b) Aharonov-Bohm periodic oscillations, with the first two harmonics directly visible in the $G(B_{\parallel})$ trace; (c) fast-Fourier transform revealing higher-order harmonics, up to $n = 6$ at very low temperature. After [39].

3.3. Quantum coherence II: non-universal conductance fluctuations

More information about the weak scattering of quantized surface modes by a non-magnetic disorder can be obtained by studying the (static) conductance fluctuations due to the *longitudinal motion* of surface carriers in a highly-disordered 3DTI quantum wire. Contrary to the case of a diffusive mesoscopic conductor, their statistical properties such as the conductance variance are not universal and they can vary when the quantized Dirac band structure is modified by an Aharonov-Bohm flux [18]. Using a 3D vector magnet, we could vary independently the longitudinal field (tuning of the energy spectrum; transverse motion) and the transverse magnetic field (probing the aperiodic conductance fluctuations due to disorder; longitudinal motion). This provides the complete mapping of quantum interference, as seen in **Figure 8a**). It was shown that the absolute amplitude of the conductance variance $\text{var}G = \delta G_{\text{rms}}^2 = \langle G - \langle G \rangle \rangle^2$ has a periodic modulation with the magnetic flux (**Figure 8b**), a property specific to surface transport (well-defined cross section). This behavior is well captured by numerical calculations (**Figure 8c and d**), which also reproduce the correct amplitude of this modulation $\text{mod}(\text{var}G)$. We evidenced that non-universal conductance fluctuations are the signature of the weak coupling between transverse quantized modes induced by disorder, and we inferred the amplitude of the disorder broadening Γ from the temperature dependence of the modulation $\text{mod}(\text{Var}G)$, in rather good agreement

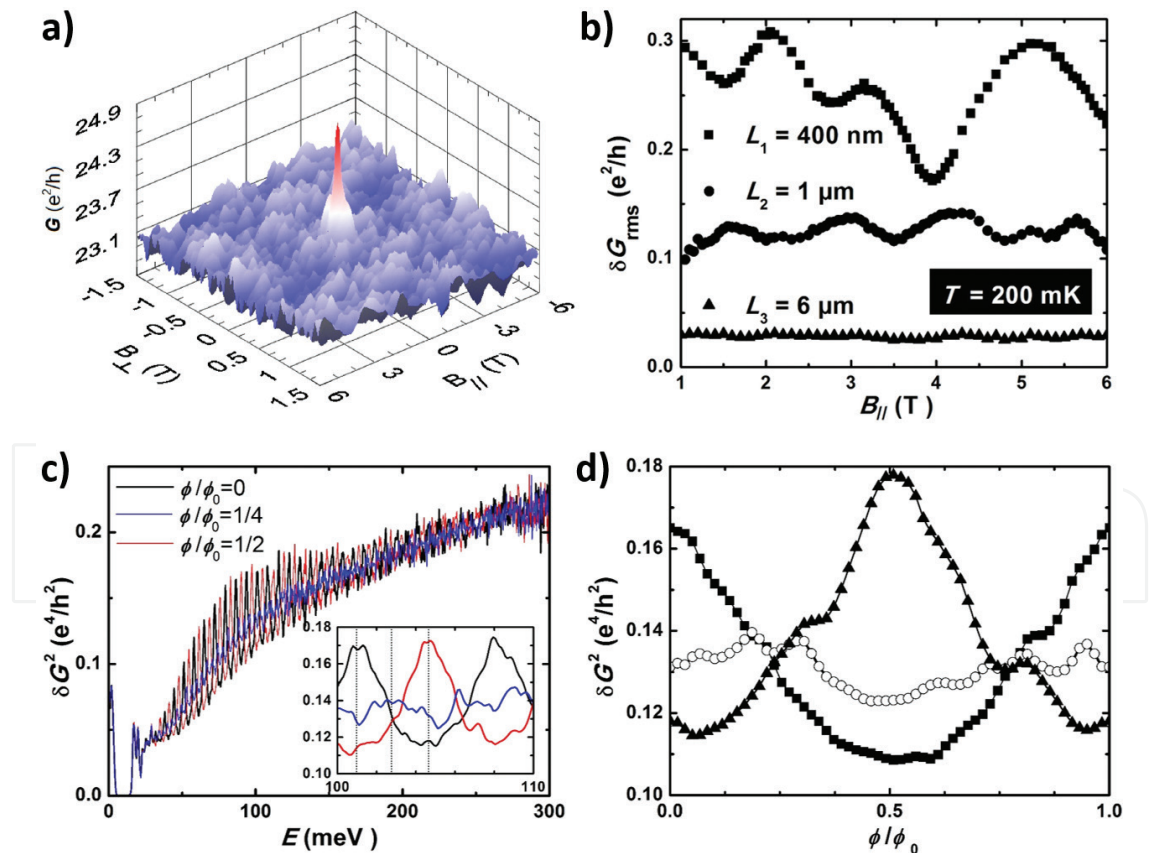


Figure 8. (a) Quantum corrections to the conductance of a Bi_2Se_3 quantum wire mapped over a large range of longitudinal magnetic fields (magnetic flux) and transverse magnetic fields, at very low temperature; (b) flux-dependence of the conductance variance revealing a non-universal behavior and a periodic evolution, a signature of the quasi-ballistic transport of Dirac surface modes; (c and d) numerical calculations of the energy (c) and flux (d) dependences of the conductance variance in a disordered 3DTI quantum wire, showing periodic evolutions due to quantum confinement of all transverse modes. After [18].

with numerical calculations [18]. Because $\Gamma \ll \Delta$, quasi-ballistic transport is a common property to all populated surface modes, each of them giving a significant contribution to the conductance (close to G_0) as compared to that of the perfect transmission case (G_0). Besides, the sharp evolution of $\text{var}G$ with the energy of successive transverse modes (**Figure 8c**) suggested that only a limited number of partially-opened modes (nearby E_F) contribute to the conductance fluctuations, due to a rapid energy dependence of the transmission for all channels.

3.4. Quasi-ballistic transport: disorder and transmissions

To evidence that this interpretation is actually very general to all quantum corrections to the conductance in 3DTI quantum wires, it is important to calculate the energy dependence of the transmissions for all modes, taking disorder into account but also interfaces with metallic contacts. This was done in a comparative study of numerical calculations with an analytical model that captures the main property common to all quasi-1D spin-helical surface modes, that is, the suppression of scattering due to quantum confinement [41]. The set of transmissions T_i represents the mesoscopic code of a coherent conductor, from which all important quantities can be calculated [45], the simplest one being the total conductance $G = \sum T_i G_0$. Importantly, the transmissions were found to nearly reach unity for all modes when their longitudinal kinetic energy exceeds Δ (**Figure 9**). The same (rapid) evolution was found even for high-energy modes, though over a slightly broader energy window, thus explaining why quasi-ballistic transport properties exist for many modes over a broad energy range. This also shows that diffusive longitudinal transport is realized only for conductor lengths that largely exceed the transport length. Contrary to the case of 2D quasi-particles with isotropic scattering for which the transition from the ballistic to the diffusive regime is rather abrupt ($l_e < L < L_{tr}$ with $L_{tr} \leq 2l_e$), the quasi-ballistic regime in 3DTI quantum wires exists over a wider parameter range ($L_{tr}/2 < L < \alpha L_{tr}$ with $L_{tr} \gg l_e$ and α is related to the aspect ratio L/L_p). This unusual behavior, related to the enhanced transport length, is due to both the spin texture of Dirac modes (anisotropic scattering) and to their large confinement energy in quantum wires, both favoring the weak scattering of quantized modes by disorder.

3.4.1. Scattering by disorder and contacts

Considering the scattering by disorder as due to a random potential of energy barriers (Gaussian disorder, with a correlation length ξ , see **Figure 10a**), it is possible to give an analytical description of the transmissions of high-energy modes propagating between two transparent ohmic contacts, for different degrees of disorder from the clean limit (ballistic, Fabry-Pérot) to the dirty limit (diffusive) [41]. In the quasi-ballistic regime, we found that the conductance is determined by the interfaces with metallic contacts (similarly to a clean conductor) and not by details of the microscopic disorder in the quantum wire. Due to the quantum confinement of Dirac fermions with evenly-spaced energy levels, the energy dependence of the conductance can oscillate at low energies (whereas it has a linear dependence at high energy, as for the 2D limit) and the average transmission per mode only depends on the nature of the contacts. For an intermediate disorder strength g , Fabry-Pérot interferences are suppressed by efficient phase averaging, and inter-mode scattering results in an oscillatory energy dependence of the transmission, due to the increased density of states at the onset of a

nearby mode and because disorder broadening remains smaller than the energy level spacing. This can be directly seen in the energy dependence of the transmission of a high-energy mode in a Bi_2Se_3 quantum wire (using a realistic value of ξ), as shown in **Figure 10b**). For very large values of g , Γ exceeds Δ and charge transport becomes diffusive.

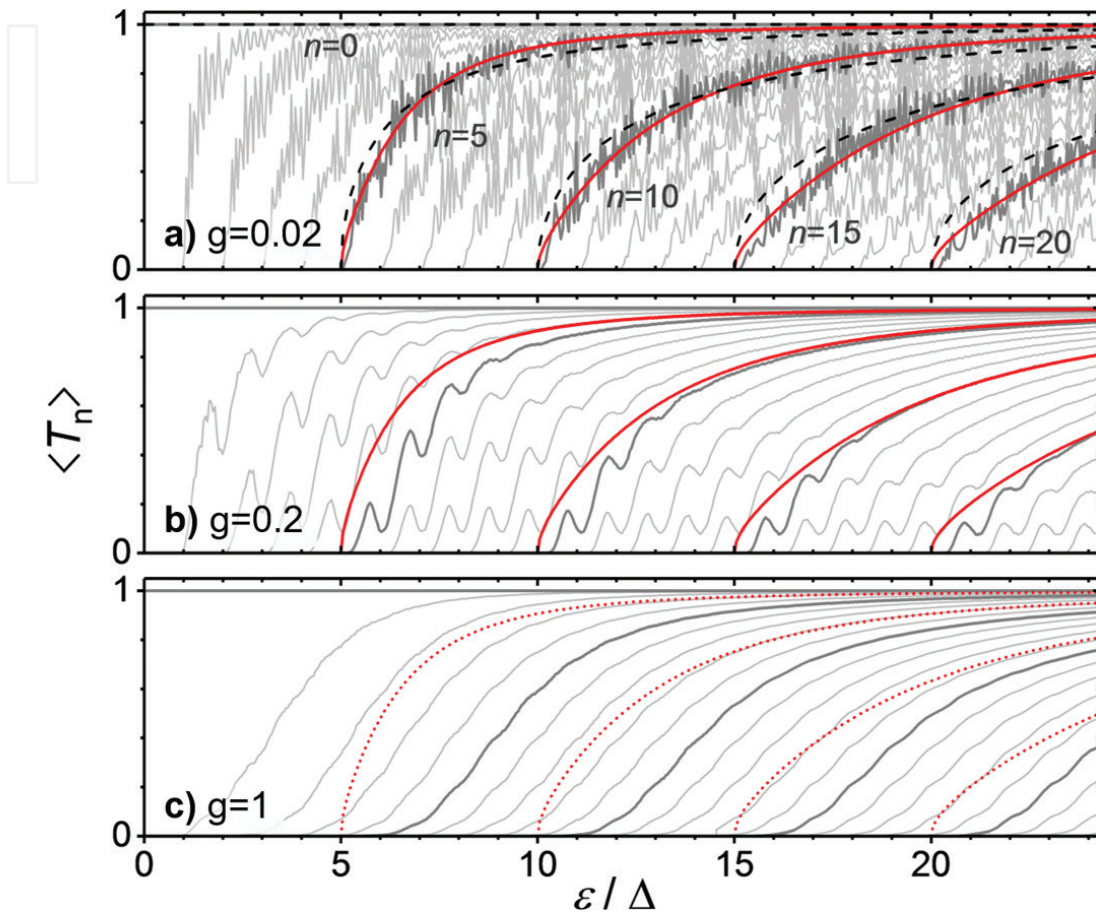


Figure 9. Energy dependence of the surface-mode transmissions in disordered 3D topological insulator quantum wires, for three values of the disorder strength $g=0.02$ (a), $g=0.2$ (b), and $g=1$ (c). After [41].

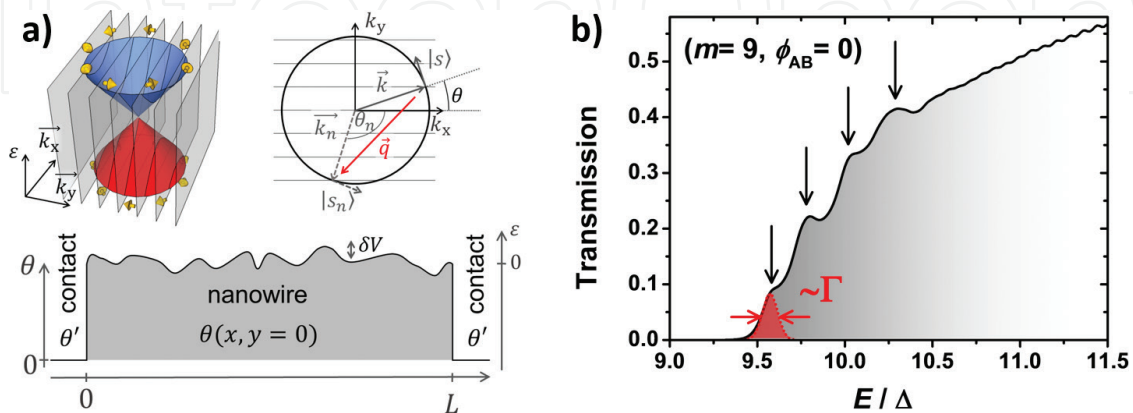


Figure 10. (a) Quantized band structure of surface modes for a magnetic flux $\phi = 1/2\phi_0$ and inter-mode scattering induced by a random disorder potential δV ; (b) energy dependence of the transmission of the $m = 9$ quantized mode for $\phi = 0$, showing resonances due to disorder-induced inter-mode mixing, with an energy broadening Γ . After [41].

To understand why the quasi-ballistic regime exists over a broad range of parameters, it is important to consider the energy dependence of the transport length [see [41] for details], as shown in **Figure 11** for different g values. Contrary to the case of massive quasi-particles, L_{tr} does not vanish at low energy for Dirac fermions in 1D. Instead, it diverges and a similar behavior occurs at high energy, due to the anisotropy of scattering. As a consequence, the transport length has a minimum value that depends on the strength of disorder. For a given disorder correlation length ξ , this minimum value is obtained for $k\xi \approx 1$ and the values of L_{tr}^{\min} can be much larger than the transverse dimensions of the nanostructure for all energies, for a broad range of g values, so that the condition for quasi-ballistic transport is always fulfilled for such highly-disordered 3D topological insulator quantum wires. Good agreement was found between this simplified analytical model and numerical calculations, for that details of the microscopic disorder do not affect the conductance in this regime, which is mostly determined by metallic contacts.

3.4.2. Quantitative derivation of the Aharonov-Bohm amplitude

Based on the transmissions calculated for different values of the magnetic flux (corresponding to different quantized energy spectra), it is possible to calculate the energy dependence of Aharonov-Bohm oscillations. As seen in **Figure 11**, their amplitude decreases with the energy of surface modes and a good quantitative agreement with experiments are found at high energies. The oscillatory behavior reported in experiments is also well reproduced, as well as energy-periodic phase shifts [33] which are actually due to the quantized band structure (**Figure 12**) [41].

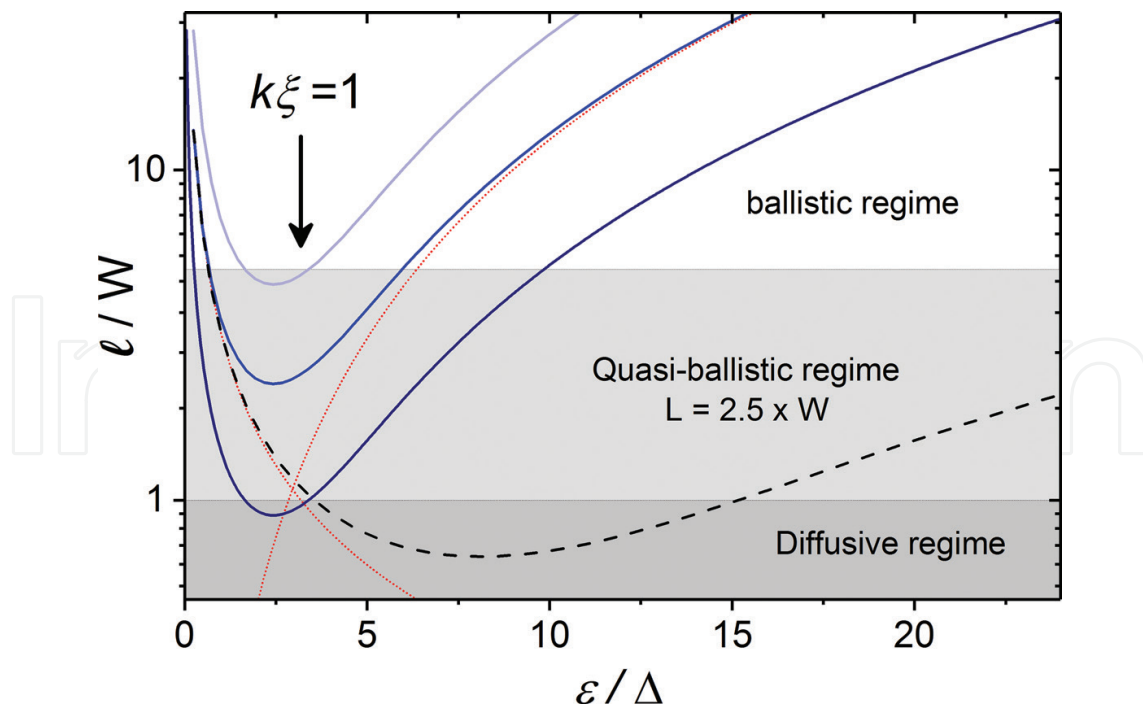


Figure 11. Energy dependence of the transport length l in a quantum wire with a perimeter $W = L_p$ and a transverse energy quantization Δ is calculated for three different strengths of the disorder potential. Red dotted lines show asymptotic behaviors related to the divergence of $l = L_{tr}$ at low or high energies, due to the density of states or to the anisotropy of scattering, respectively. In all cases, the transport of all surface modes is ballistic or quasi-ballistic. After [41].

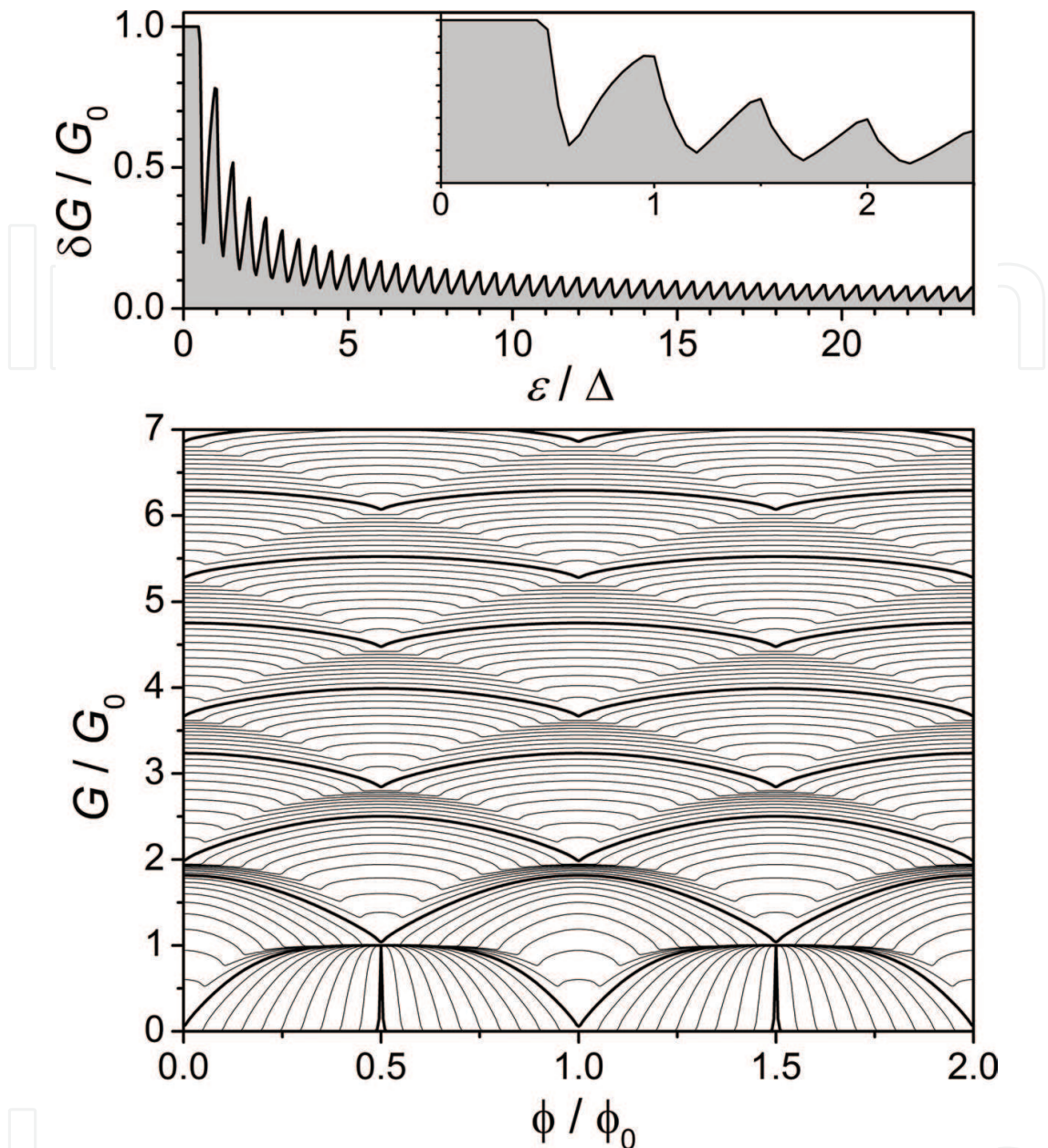


Figure 12. (a) Energy dependence of the Aharonov-Bohm amplitude, rapidly decreasing from the conductance quantum G_0 (contribution of the topological mode only) to a fraction of G_0 (contribution of higher-energy transverse modes); (b) flux dependence of the conductance for different energies, from 0 to 4.5Δ (successive thin lines correspond to an energy change 0.05Δ and thick lines to multiple values of $1/2 \Delta$). Phase shifts are due to the quantized energy spectrum of surface modes. The influence of the topological mode is seen only for very low energies. After [41].

3.4.3. Perfectly-transmitted topological mode

To evidence the influence of the topological mode on the conductance, it is therefore necessary to set the mesoscopic conductor in specific conditions:

1. In long wires, the transmission of all modes but the topological one should be reduced. However, the spin texture of surface Dirac states prevents the strong localization of

high-energy modes, so that this is not a good strategy for highly-doped quantum wires (as this is the case for Bi_2Se_3 nanostructures).

2. In the small- N limit (less than about 4–5 modes populated), the relative influence of the topological mode on the quantum magneto-conductance will be larger, also in short wires. This condition is rather restrictive and requires either to bring the electro-chemical potential close to the Dirac point or to achieve very large values of Δ .

With the goal to investigate the physics of 3D TI quantum wires close to the Dirac point, best results could be obtained in long and ultra-narrow nanostructures [46, 47], since low-energy modes other than the topological mode have a reduced transmission due to disorder (minimum of the backscattering length, so that $L_{\text{tr}} \ll L$ and $G \ll G_0$). Furthermore, since the transport of surface modes is quasi-ballistic, it will become important to optimize/control the coupling between metallic contacts and the transverse wave function of a given mode. In particular, the amplitude of probability can have an azimuthal angle dependence, which varies from one mode to another, so that quantum transport properties will ultimately depend on the exact geometry of the mesoscopic conductor. Also, the low-energy spectrum can be modified by a large transverse magnetic field. For a rectangular cross section (**Figure 13**), a striking property is related to the evolution of the topological mode from a helical state to a chiral edge state, when a moderate transverse magnetic field is applied [42]. The specific orbital response of such 3DTI quantum wires corresponds to an intermediate situation between the quantum spin Hall in a 2D TI and the Quantum Hall effect in 2DEGs.

The control of low-energy quantum states in 3DTI nanostructures would offer novel opportunities for their quantum manipulation as well as for spin filtering, tuning the quantum states with an electric or a magnetic field. When coupled to metallic electrodes with gapped excitations, the topological mode generates novel quantum states with an intrinsic topological protection, such as Majorana bound states or spin-polarized edge states in the quantum

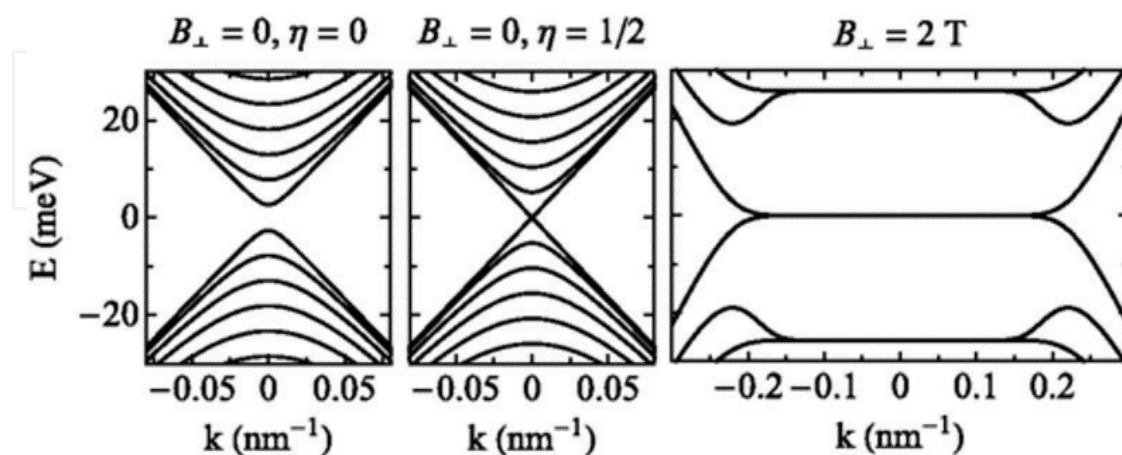


Figure 13. Energy spectrum of a 3DTI quantum wire with a rectangular cross section ($h = 40$ nm; $w = 160$ nm) for $\eta = \phi/\phi_0 = 0$ (left) and $\eta = \phi/\phi_0 = 1/2$ (center; right), low-energy band structure in the presence of a large transverse magnetic induction $B_{\perp} = 2$ T, showing the emergence of chiral edge states without dispersion over a wide range of impulse, independent of η . After [42].

anomalous Hall regime. These could be important for quantum dynamics studies, with limited decoherence. Non-topological low-energy modes are also interesting for their energy tuning, by a gate voltage or a magnetic flux, which is associated with a continuous change of their spin state between nearly-orthogonal states. Besides, these can be either 1D extended states (long quantum wires) or 0D localized states (short quantum wires, that is, for $L < L_{tr}$).

4. Conclusion and perspectives

The weak coupling of surface states in 3D topological insulator quantum wires, due to both their spin texture and the quantum confinement of Dirac fermions, gives unique opportunities to control novel quantum states in mesoscopic conductors, despite non-magnetic disorder. Yet, it remains difficult to control a small number of transverse quantized states close to the Dirac degeneracy point, mostly due to intrinsic limitations in conventional 3DTIs materials. Whereas the Bi_2Se_3 family offers many advantages (tunable band structure in solid solutions of ternary compounds and high-quality single-crystalline nanostructures), it remains difficult to achieve surface transport only, and, most important, to control low-energy surface quasi-particles (large residual bulk doping or interface charge transfer, due to disorder).

Therefore, the next generation of electronic devices based on 3D topological insulators will necessarily be developed from advanced functional nanostructures and heterostructures. One of the most important challenge will be the full control of interface band bending, with a high-enough interface quality so as to optimize the coupling between metallic contacts and spin-helical surface Dirac fermions. For instance, this is particularly true for spin transport experiments, which require to minimize the momentum/spin relaxation below the contacts in order to make use of the intrinsic potential of electronic states with spin-momentum locking.

Toward this goal, new growth and nanofabrication methods need to be envisioned, in combination with those already used to prepare high-quality single-crystalline nanostructures (vapor transport, vapor-liquid-solid epitaxy, and chemical-vapor deposition). Novel techniques, such as the in-situ stencil lithography of metallic contacts combined the growth of ultra-thin films by molecular beam epitaxy, already gave some promising results, for instance to realize highly-transparent superconducting contacts and investigate topological superconductivity [48]. Also, atomic layer epitaxy holds promises to realize core-shell lateral nanostructures adapted to the control of the electro-chemical potential at the interface with a topological insulator [49–51].

Acknowledgements

This work was supported by the German Research Foundation DFG through the SPP 1666 Topological Insulators program. This book chapter reviews our previous work on 3D topological insulator quantum wires, for which we acknowledge the contributions of our collaborators: J. H. Bardarson, B. Büchner, J. Cayssol, B. Dassonneville, B. Eichler, W. Escoffier, H. Funke, S. Hampel, C. Nowka, O.G. Schmidt, J. Schumann, L. Veyrat, K. Wruck, and E. Xypakis.

Conflict of interest

The authors declare no conflict of interest.

Author details

Romain Giraud^{1,2*} and Joseph Dufouleur²

*Address all correspondence to: romain.giraud@cea.fr

1 Univ. Grenoble Alpes, CNRS, CEA, Grenoble-INP, Institute of Engineering Univ. Grenoble Alpes, INAC-Spintec, Grenoble, France

2 Leibniz Institute for Solid State and Materials Research, IFW Dresden, Dresden, Germany

References

- [1] Hasan MZ, Kane CL. Topological insulators. *Reviews of Modern Physics*. 2010;**82**:3045
- [2] Qi X-L, Zhang S-C. Topological insulators and superconductors. *Reviews of Modern Physics*. 2011;**83**:1057
- [3] Bernevig BA, Zhang S-C. Quantum spin Hall effect. *Physical Review Letters*. 2006;**96**:106802
- [4] Kane CL, Mele EJ. Quantum spin Hall effect in Graphene. *Physical Review Letters*. 2005;**95**:226801. DOI: <https://doi.org/10.1103/PhysRevLett.95.226801>
- [5] Büttiker M. Edge-state physics without magnetic fields. *Science*. 2009;**325**:278. DOI: [10.1126/science.1177157](https://doi.org/10.1126/science.1177157)
- [6] Fu L, Kane CL, Mele EJ. Topological insulators in three dimensions. *Physical Review Letters*. 2007;**98**:106803
- [7] Moore JE, Balents L. Topological invariants of time-reversal-invariant band structures. *Physical Review B*. 2007;**75**:121306. DOI: <https://doi.org/10.1103/PhysRevB.75.121306>
- [8] Culcer D, Hwang EH, Stanescu TD, Das Sarma S. Two-dimensional surface charge transport in topological insulators. *Physical Review B*. 2010;**82**:155457
- [9] Kane CL, Mele EJ. Z₂ topological order and the quantum spin Hall effect. *Physical Review Letters*. 2005;**95**:146802
- [10] Fu L, Kane CL. Superconducting proximity effect and Majorana fermions at the surface of a topological insulator. *Physical Review Letters*. 2008;**100**:096407
- [11] Oh S. The complete quantum Hall trio. *Science*. 2013;**340**:153

- [12] König M, Wiedmann S, Brüne C, Roth A, Buhmann H, Molenkamp LW, Qi X-L, Zhang S-C. Quantum spin Hall insulator state in HgTe quantum wells. *Science*. 2007;**318**:766-770. DOI: 10.1126/science.1148047
- [13] Bernevig BA, Zhang S-C. Quantum spin Hall effect. *Physical Review Letters*. 2006;**96**:106802
- [14] Chen YL, Analytis JG, Chu J-H, Liu ZK, Mo S-K, Qi XL, Zhang HJ, Lu DH, Dai X, Fang Z, Zhang SC, Fisher IR, Hussain Z, Shen Z-X. *Science*. 2009;**325**:178
- [15] Hsieh D, Xia Y, Qian D, Wray L, Dil JH, Meier F, Osterwalder J, Patthey L, Checkelsky JG, Ong NP, Fedorov AV, Lin H, Bansil A, Grauer D, Hor YS, Cava RJ, Hasan MZ. *Nature (London)*. 2009;**460**:1101
- [16] Xia Y, Qian D, Hsieh D, Wray L, Pal A, Lin H, Bansil A, Grauer D, Hor YS, Cava RJ, Hasan MZ. *Nature Physics*. 2009;**5**:398
- [17] Dufouleur J, Veyrat L, Dassonneville B, Nowka C, Hampel S, Leksin P, Eichler B, Schmidt OG, Büchner B, Giraud R. Enhanced mobility of spin-helical Dirac fermions in disordered 3D topological insulators. *Nano Letters*. 2016;**16**:6733
- [18] Dufouleur J, Veyrat L, Dassonneville B, Xypakis E, Bardarson JH, Nowka C, Hampel S, Eichler B, Schmidt OG, Büchner B, Giraud R. Weakly-coupled quasi-1D helical modes in disordered 3D topological insulator quantum wires. *Scientific Reports*. 2017;**7**:45276
- [19] Dankert A, Geurs J, Kamalakar MV, Charpentier S, Dash SP. Room temperature electrical detection of spin polarized currents in topological insulators. *Nano Letters*. 2015;**15**:7976
- [20] Jamali M, Lee JS, Jeong JS, Mahfouzi F, Lv Y, Zhao Z, Nikolić BK, Mkhoyan KA, Samarth N, Wang J-P. Giant spin pumping and inverse spin Hall effect in the presence of surface and bulk spin-orbit coupling of topological insulator Bi₂Se₃. *Nano Letters*. 2015;**15**:7126
- [21] Lee JS, Richardella A, Hickey DR, Mkhoyan KA, Samarth N. Mapping the chemical potential dependence of current-induced spin polarization in a topological insulator. *Physical Review B*. 2015;**92**:155312
- [22] Li CH, vant Erve OM, Robinson JT, Liu Y, Li L, Jonker BT. Electrical detection of charge-current-induced spin polarization due to spin-momentum locking in Bi₂Se₃. *Nature Nanotechnology*. 2014;**9**:218
- [23] Mellnik AR, Lee JS, Richardella A, Grab JL, Mintun PJ, Fischer MH, Vaezi A, Manchon A, Kim E-A, Samarth N, Ralph DC. Spin-transfer torque generated by a topological insulator. *Nature*. 2014;**511**:449
- [24] Pesin D, MacDonald AH. Spintronics and pseudospintronics in graphene and topological insulators. *Nature Materials*. 2012;**11**:409
- [25] Rojas-Sánchez JC, Oyarzun S, Fu Y, Marty A, Vergnaud C, Gambarelli S, Vila L, Jamet M, Ohtsubo Y, Taleb-Ibrahimi A, Le Fevre P, Bertran F, Reyren N, George J-M, Fert A. Spin to charge conversion at room temperature by spin pumping into a new type of topological insulator: α -Sn films. *Physical Review Letters*. 2016;**116**:096602

- [26] MÜchler L, Casper F, Yan B, Chadov S, Felser C. Topological insulators and thermoelectric materials. *Physica Status Solidi RRL*. 2013;**7**:91-100. DOI: <https://doi.org/10.1002/pssr.201206411>
- [27] Cava RJ, Ji H, Fuccillo MK, Gibson QD, Hor YS. Crystal structure and chemistry of topological insulators. *Journal of Materials Chemistry C*. 2013;**1**:3176
- [28] Brahlek M, Koirala N, Bansal N, Oh S. Transport properties of topological insulators: Band bending, bulk metal-to-insulator transition, and weak anti-localization. *Solid State Communications*. 2015;**215-216**:54-62. DOI: 10.1016/j.ssc.2014.10.021
- [29] Zhang J et al. Band structure engineering in $(\text{Bi}_{1-x}\text{Sbx})_2\text{Te}_3$ ternary topological insulators. *Nature Communications*. 2011;**2**:574
- [30] Xu Y, Miotkowski I, Liu C, Tian J, Nam H, Alidoust N, Hu J, Shih C-K, Hasan MZ, Chen YP. Observation of topological surface state quantum Hall effect in an intrinsic three-dimensional topological insulator. *Nature Physics*. 2014;**10**:956-963. DOI: 10.1038/nphys3140
- [31] Bässler S, Hamdou B, Sergelius P, Michel A-K, Zierold R, Reith H, Gooth J, Nielsch K. One-dimensional edge transport on the surface of cylindrical $\text{Bi}_x\text{Te}_{3-y}\text{Se}_y$ nanowires in transverse magnetic fields. *Applied Physics Letters*. 2015;**107**(18):181602
- [32] Hong SS, Zhang Y, Cha JJ, Qi X-L, Cui Y. One-dimensional helical transport in topological insulator nanowire interferometers. *Nano Letters*. 2014;**14**:2815
- [33] Jauregui LA, Pettes MT, Rokhinson LP, Shi L, Chen YP. Magnetic field-induced helical mode and topological transitions in a topological insulator nanoribbon. *Nature Nanotechnology*. 2016;**11**:345
- [34] Renard VT et al. Quantum corrections to the conductivity and Hall coefficient of a two-dimensional electron gas in a dirty AlGaAs/GaAs/AlGaAs quantum well: From the diffusive to the ballistic regime. *Physical Review B*. 2005;**72**:075313
- [35] Niimi Y et al. Quantum coherence at low temperatures in mesoscopic systems: Effect of disorder. *Physical Review B*. 2010;**81**:245306
- [36] Veyrat L, Iacovella F, Dufouleur J, Nowka C, Funke H, Yang M, Escoffier W, Goiran M, Eichler B, Schmidt OG, Büchner B, Hampel S, Giraud R. Band bending inversion in Bi_2Se_3 nanostructures. *Nano Letters*. 2015;**15**:7503
- [37] Nowka C, Veyrat L, Gorantla S, Steiner U, Eichler B, Schmidt OG, Funke H, Dufouleur J, Büchner B, Giraud R, Hampel S. Catalyst-free growth of single-crystalline Bi_2Se_3 nanostructures for quantum transport studies. *Crystal Growth & Design*. 2015;**15**:4272
- [38] Xu Y, Miotkowski I, Chen YP. Quantum transport of two-species Dirac fermions in dual-gated three-dimensional topological insulators. *Nature Communications*. 2016;**7**:11434
- [39] Dufouleur J, Veyrat L, Teichgräber A, Neuhaus S, Nowka C, Hampel S, Cayssol J, Schumann J, Eichler B, Schmidt OG, Büchner B, Giraud R. Quasiballistic transport of Dirac fermions in a Bi_2Se_3 nanowire. *Physical Review Letters*. 2013;**110**:186806

- [40] Peng H, Lai K, Kong D, Meister S, Chen Y, Qi X-L, Zhang S-C, Shen und Z-X, Cui Y. Aharonov-Bohm interference in topological insulator nanoribbons. *Nature Materials*. 2010;**9**(3):225-229
- [41] Dufouleur J, Xypakis E, Büchner B, Giraud R, Bardarson JH. Suppression of scattering in quantum confined 2D-helical Dirac systems. *Physical Review B*. 2018;**97**:075401
- [42] De Juan F, Ilan R, Bardarson JH. Robust transport signatures of topological superconductivity in topological insulator nanowires. *Physical Review Letters*. 2014;**113**:107003
- [43] Bardarson JH, Brouwer PW, Moore JE. Aharonov-Bohm oscillations in disordered topological insulator nanowires. *Physical Review Letters*. 2010;**105**:156803
- [44] Cho S, Dellabetta B, Zhong R, Schneeloch J, Liu T, Gu G, Gilbert MJ, Mason N. Aharonov-Bohm oscillations in a quasi-ballistic three-dimensional topological insulator nanowire. *Nature Communications*. 2015;**6**:7634
- [45] Akkermans E, Montambaux G. *Mesoscopic Physics of Electrons and Photons*. 1st ed. Cambridge, England: Cambridge University Press; 2007
- [46] Krieg J, Chen C, Avila J, Zhang Z, Sigle W, Zhang H, Trautmann C, Asensio und MC, Toimil-Molares ME. Exploring the electronic structure and chemical homogeneity of individual Bi₂Te₃ nanowires by nano-angle-resolved photoemission spectroscopy. *Nano Letters*. 2016;**16**(7):4001-4007
- [47] Krieg J, Funke H, Giraud R, Dufouleur J, Trautmann C, Büchner B, Toimil-Morales E. Magnetotransport measurements on Bi₂Te₃ nanowires electrodeposited in etched ion-track membranes. *Journal of Physics and Chemistry of Solids*. (Accepted)
- [48] Schüffelgen P et al. Stencil lithography of superconducting contacts on MBE-grown topological insulator thin films. *Journal of Crystal Growth*. 2017;**477**:183-187
- [49] Hamdou B, Gooth J, Böhnert T, Dorn A, Akinsinde L, Pippel E, Zierold R, Nielsch K. Thermoelectric properties of band structure engineered topological insulator (Bi_{1-x}Sb_x)₂Te₃ nanowires. *Advanced Energy Materials*. 2015;**5**:1500280
- [50] Murakami S, Nagaosa N, Zhang S-C. Spin-Hall insulator. *Physical Review Letters*. 2004;**93**:156804
- [51] Pankratov OA, Pakhomov SV, Volkov BA. Supersymmetry in heterojunctions: Band-inverting contact on the basis of Pb_{1-x}Sn_xTe and Hg_{1-x}Cd_xTe. *Solid State Communications*. 1987;**61**:93-96. DOI: 10.1016/0038-1098(87)90934-3

